

# Biogenic nanosilver from *Cornus mas* fruits as multifunctional eco-friendly platform: “green” development and biophysical characterization

M. E. BARBINTA-PATRASCU\*

University of Bucharest, Faculty of Physics, 405 Atomistilor Street, PO Box MG-11, Bucharest-Magurele, 077125, Romania

The idea to use „green” nano-approaches in many fields such as: bioelectronics, biophotonics, or nanomedicine is in the spotlight of scientific world nowadays. This work aimed to highlight novel applications of silver nanoparticles “green” synthesized from *Cornus mas* L. fruits aqueous extract. Dynamic Light Scattering (DLS) results revealed the achieving of AgNPs with a diameter of 41.5 nm. Bio-resulted AgNPs presented moderate physical stability (ZP = -23.25 mV) and demonstrated binding capacity to DNA molecule, fact confirmed by UV-Vis absorption spectroscopy. The strong bathochromic shift of SPR band of cornelian-derived AgNPs could be exploited in DNA biosensing applications. Electrical conductivity measurements revealed the urease inhibitory action of these AgNPs. These findings show that developed nano-bio-silver particles proved to have potential use in biomedical field (urease inhibitor, Drug Delivery Systems design), in biophotonics or in biosensing applications.

(Received September 29, 2020; accepted October 22, 2020)

**Keywords:** Biogenic AgNPs, DNA binding, Urease inhibitor, Spectral characterization, Electrical conductivity

## 1. Introduction

In the last years, special attention was paid to develop novel „green” nano-strategies to fight against diseases or to design valuable devices for bioelectronics or biophotonics, by combining bio-organic matter with inorganic ones. Thus, valorization of huge potential of plants and vegetal wastes to „green” synthesis metallic nanoparticles is a current trend in nanotechnology.

Plant extracts are getting more attention due to low-cost and low toxicity, and have been exploited for application in photonics [1] or as precursors for „green” designing various nanomaterials with great potential in biomedical field, biosensing, and biophotonics [2-7].

In this study, silver nanoparticles (AgNPs) phytosynthesized from aqueous extract of *Cornus mas* L. fruits were assayed as urease inhibitors and as DNA binders for Drug Delivery Systems design or DNA biosensing applications. These “green” AgNPs were used in the author previous works to generate antioxidant and antimicrobial nanobioarchitectures [8-9], the cornelian cherries being known to possess antioxidant and antibacterial properties due to their high content of bioactive phyto-compounds (ascorbic acid, polyphenols, anthocyanins and carotenoids) [8-9].

DNA is the “smart” biological molecule, which stores, transmits, and translates the genetic information for development and functioning of all living organisms. Its unique architecture consisting of two polynucleotide strands that adopt helical duplex structure based on the classical Watson–Crick base pairing interactions, allows interactions with itself or with other biomolecules

(proteins, lipids) or with biomimetic membranes [10], or with photosensitive molecules [11-15] and metallic nanoparticles giving rise to materials having applications in various fields [16].

Moreover, various phytochemicals (curcumin, luteolin, piperine, and gingerol) were exploited for binding studies on biomacromolecules [17] to control various diseases by improving the strategies in drug designing.

In the last decades, the phytosynthesized precious metal nanoparticles (AgNPs and AuNPs) have fascinated through their unique properties like antioxidants, antimicrobial, anticancer agents and DNA binders, being used in cancer treatment [18]. Liu and Huang [19] prepared DNA–AgNPs complexes for the quantitative detection of HIV DNA. Other researchers reported studies of various metallic nanoparticles conjugated with DNA of interest in sensor development and electronic applications [18].

In this research, UV-Vis absorption spectroscopy was employed to study the binding of the obtained cornelian AgNPs on DNA molecule. The size of the biosynthesized AgNPs was estimated by Dynamic Light Scattering (DLS), and their physical stability by zeta potential measurements.

Furthermore, the obtained AgNPs were investigated for the urease inhibitory action, by electrical conductivity measurements. The reasons for studying the effect of the phytosynthesized AgNPs on urease activity, are further detailed.

The usual urease inhibitors obtained through chemical synthesis undergone degradation process in time and breakdown products could be toxic to environment, and

hence, the use of “green” urease inhibitors are more attractive.

Urease (urea amidohydrolase, EC 3.5.1.5) is a nickel-containing enzyme common in nature, which is present in animals, plants, microorganisms (fungi, and bacteria) and in soils (soil ureases come from syntheses realized by microorganisms and plant materials). This enzyme catalyzes the hydrolysis of urea into ammonia and carbamate, and it has historical importance in Biochemistry, being the first enzyme ever to be crystallized (1926) [20].

Urea, the enzymatic substrate of urease, is the most widely used nitrogen fertilizer, but after its application to soil, urea undergoes hydrolysis *via* the urease enzyme, causing increases in the soil pH, and resulting in NH<sub>3</sub> losses to the atmosphere, being an economic problem (because less nutrient is left for plants to take up, affecting crop yields), and an environmental concern [21].

Moreover, urease has been reported to contribute to the pathogenesis of pyelonephritis, urolithiasis, encephalopathy, hepatic coma, gastritis and gastric ulcer [22]. It is necessary to mention that urease secreted by *Helicobacter pylori* is a crucial enzyme able to allow bacteria to colonize and survive in acidic environment of the human stomach [23].

Therefore, there is a tremendous interest to find eco-friendly urease inhibitors which delay or block the urea hydrolysis. The use of plant extracts as urease inhibitors was recently highlighted for Neem oil and neem cake extracted from *Azadirachta indica* [21], *Hibiscus sabdariffa* L. [22], *Citrus* fruits [23], and *Salvia officinalis* [24].

Modolo *et al.* reviewed that the use of AgNPs as additive in urea-based formulations decreased urease activity, and could be advantageous to contribute for pest control in agriculture [25].

In this study, “green” synthesized AgNPs were investigated for the anti-urease activity, by electrical conductivity measurements.

## 2. Experimental part

### 2.1. Materials

Herring DNA was purchased from Fluka (Switzerland), and sodium chloride (NaCl) from Sigma Aldrich (Germany). Sodium hydrogen phosphate (Na<sub>2</sub>HPO<sub>4</sub>) and potassium dihydrogen phosphate (KH<sub>2</sub>PO<sub>4</sub>) were acquired from Merck (Germany).

All other chemicals were supplied from Gatt Koller-GmbH (Austria).

*Cornus mas* L. fruits were acquired from a local market.

### 2.2. Green Synthesis of Silver Nanoparticles (bio-AgNPs)

Cornelian cherries aqueous extract was used as a precursor for the synthesis of AgNPs by acting both as a

bio-reducing of silver ions and a capping agent for resulted AgNPs. The phytosynthesis was conducted as previously described [8-9]. Briefly, an appropriate amount of fresh *Cornus mas* fruits were added into hot distilled water, in a mass ratio of 1:10 (w/w), and then boiled for 5 minutes, cooled at room temperature and finally filtered through a filter paper in order to obtain a clear red extract.

Equal volumes of cornelian extract and 1 mM AgNO<sub>3</sub> aqueous solution were mixed. After a while, the colour of *C. mas* extract turned to dark reddish brown with mirror-like illumination explained by the excitation of surface plasmon vibrations in the resulting silver nanoparticles (bio-AgNPs).

### 2.3. Study of bio-AgNPs binding to DNA

DNA binding studies were carried out in physiological conditions, at  $t = 37^{\circ}\text{C}$  and in phosphate saline buffer (PBS) at pH 7.4.

The concentration of herring DNA solution prepared in PBS pH 7.4, was calculated from UV absorption spectrum, according to the absorbance at 260 nm by using the Lambert-Beer law (the molar absorption coefficient for DNA:  $\epsilon_{260} = 6600 \text{ M}^{-1}\text{cm}^{-1}$ ) [15].

Increasing amounts of bio-AgNPs were gradually added to DNA solution and UV-Vis absorption spectra were recorded each time.

### 2.4. Investigation of urease inhibitory activity of “green” synthesized AgNPs

Urease inhibitory activity of AgNPs was evaluated by electrical conductivity measurements, using Cobra3 Chem-Unit experimental set-up, containing a conductivity electrode (Phywe Systeme GmbH, Göttingen).

The following solutions were used in these experiments: (i) urease solution in 50% glycerine (1000 U/mL) and (ii) 1.6% urea solution in distilled water.

Urease is the enzyme which catalyzes the urea hydrolysis resulting in ammonia and carbon dioxide. The ions of the reaction products increase the medium conductivity, so the conductivity measurements are closely correlated to the rate of the urea hydrolysis reaction.

To a volume of 40 mL of 1.6% urea solution, was added 50  $\mu\text{L}$  urease solution.

In this study, appropriate volumes of the prepared bio-AgNPs suspension were added in the reaction medium, and it was compared the rate in absence and in presence of bio-AgNPs. The rate of the urea hydrolysis reaction was calculated as variation in time of conductivity.

### 2.5. Characterization methods

The UV-Vis absorption spectra were obtained using a double beam spectrophotometer Lambda 2S Perkin Elmer, in the wavelength range of 200-800 nm, at the resolution of 1 nm, and 0.3 nm/s scan rate.

Bio-AgNPs size was estimated by Dynamic Light Scattering (DLS) technique, on Zetasizer Nano ZS (Malvern Instruments Ltd., U.K.), at 25°C temperature and at a scattering angle of 90°. The mean hydrodynamic diameter (= the particle diameter plus the double layer thickness), and the polydispersity index – PdI (the indicative of the size distribution width;  $0 < \text{PdI} < 1$ ) for bio-AgNPs were calculated from three different measurements, and then the mean values ( $\pm$ standard deviation, SD) were reported. DLS analyses were carried out as described in [10, 26].

Zeta potential (ZP, mV) measurements were performed at 25°C, in triplicate, on Zetasizer Nano ZS (Malvern Instruments Ltd., U.K.) by applying an electric field across the aqueous suspensions of AgNPs.

### 3. Results and discussion

The obtained biogenic nanometals were characterized by DLS, and also investigated for binding to DNA molecule, and further as urease inhibitory agents.

#### 3.1. Estimation of bio-AgNPs size

The bio-AgNPs dimension distribution analyzed by DLS is displayed in Fig.1. Bio-AgNPs presented a bimodal particle size distribution with a predominant mean diameter of 41.5 nm and a polydispersity index PdI = 0.22.

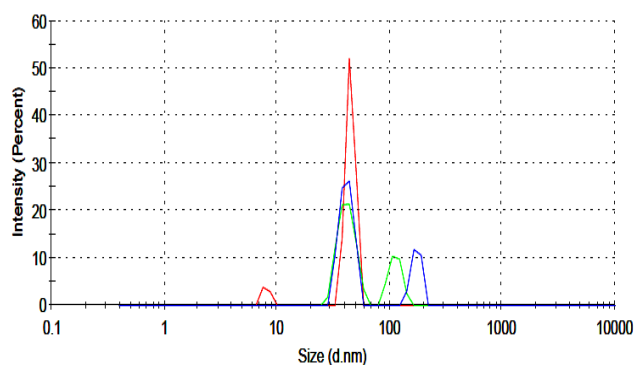


Fig. 1. Bio-AgNPs Size Distribution by Intensity, analyzed by DLS (color online)

Bio-AgNPs showed moderate physical stability, having a mean zeta potential value of ( $\text{ZP} = -23.25 \pm 0.11$  mV); this stability is assured by repulsive forces between silver nanoparticles.

#### 3.2. Optical investigation of bio-AgNPs binding to DNA molecule

The “green” developed silver nanoparticles were assayed for DNA bio-conjugation.

UV-Vis absorption spectra provided deep insight into the formation of bio-AgNPs – DNA hybrid materials.

Fig. 2 displays the absorption spectra of DNA in the absence or presence of increasing amounts of bio-AgNPs.

The equilibrium for the development of the biocomplex between DNA and bio-AgNPs is given by the following equation:



The apparent association constant ( $K_{\text{app}}$ ) was obtained from the Benesi & Hildebrand equation, as previously described [27], based on the absorption spectra of the bio-AgNPs – DNA biocomplex:

$$1/(A_{\text{obs}} - A_0) = 1/(A_C - A_0) + 1/[K_{\text{app}} \cdot (A_C - A_0) \cdot C_{\text{AgNPs}}] \quad (2)$$

where  $A_0$  is the DNA maximum absorbance in the absence of bio-AgNPs,  $A_{\text{obs}}$  is the absorbance of the sample, and  $A_C$  is the recorded absorbance at 260 nm for the DNA at different bio-AgNPs concentrations (see Fig. 2).

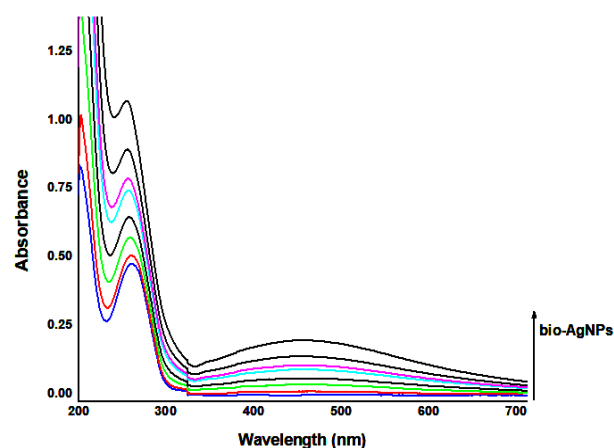


Fig. 2. The changes in the UV-Vis absorption spectra of herring DNA ( $7 \times 10^{-5}$  M) after addition of increasing amounts of bio-AgNPs ( $0 \div 7 \mu\text{M}$ ) (color online)

The plot of  $1/\Delta A = f(1/C_{\text{bio-AgNPs}})$ , where  $\Delta A = A_{\text{obs}} - A_0$ , is linear and the value of  $K_{\text{app}}$  was calculated as the ratio of the intercept to the slope (Fig. 3), and it was found to be  $9 \times 10^3 \text{ M}^{-1}$ , confirming the formation of the bio-AgNPs–DNA biocomplex.

Addition of increasing amounts of bio-AgNPs to DNA solution, resulted in “blue” shift of the maximum characteristic for DNA and also the decrease in the height and area of this peak. This hypsochromic effect could be due to the modifications occurring in the local environment of DNA bases.

For a better visualization of these shifts, the UV-Vis absorption spectra were normalized at DNA characteristic maximum as shown in Fig. 4.

Moreover, as seen in Fig. 5, the biocomplex formation between bio-AgNPs and DNA is highlighted by a hypsochromic shift of DNA maximum peak, and a bathochromic shift of SPR band of bio-AgNPs. These “blue” and “red” shifts demonstrate the development of the biocomplex DNA-bio-AgNPs. The “red” shift

highlights that herring DNA induced bio-AgNPs agglomerations [28].

Moreover, titrating bio-AgNPs to DNA solution, resulted in hyperchromic effect of DNA maximum peak, which is due to unwinding of double-stranded DNA.

The presence of NaCl in PBS buffer reduces the repulsive forces between the negatively charged bio-AgNPs and negatively charged phosphate groups of DNA backbone, allowing the bio-AgNPs aggregation and interaction through base pairs by groove binding to DNA molecule as confirmed also by  $K_{app}$  value.

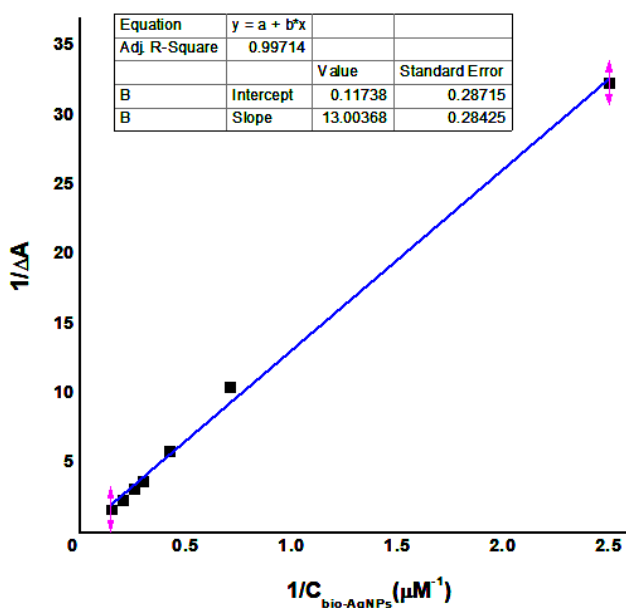


Fig. 3. Determination of apparent association constant ( $K_{app}$ ) of bio-AgNPs with herring DNA (correlation coefficient  $R^2=0.99714$ ) (color online)

Thus, the hyperchromism observed in DNA spectra after bio-AgNPs addition suggests an alteration of the secondary structure of DNA, indicating that the interaction between bio-AgNPs and DNA occurs *via* groove binding mode [29], fact confirmed also by the obtained value of binding constant which is in the order of  $10^3$ - $10^4$   $M^{-1}$  characteristic for groove binders, as compared to classical intercalators showing binding constant values on the order of  $10^7$   $M^{-1}$  [30].

“Green” synthesized AgNPs could be a promising tool to build up novel materials for possible applications in optoelectronics and biophotonics, or in drug delivery systems design.

In addition, the strong shift in the SPR band of bio-AgNPs after addition to DNA (see Fig. 4), could be exploited to develop DNA sensor systems.

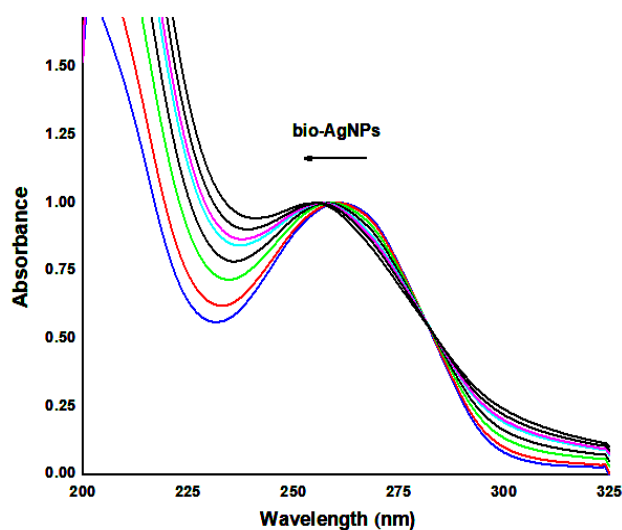


Fig. 4. Spectral shifts of DNA UV-Vis peak, with addition of increasing amounts of bio-AgNPs to DNA solution. (The absorption spectra were normalized at the characteristic DNA absorption band at 260 nm.) (color online)

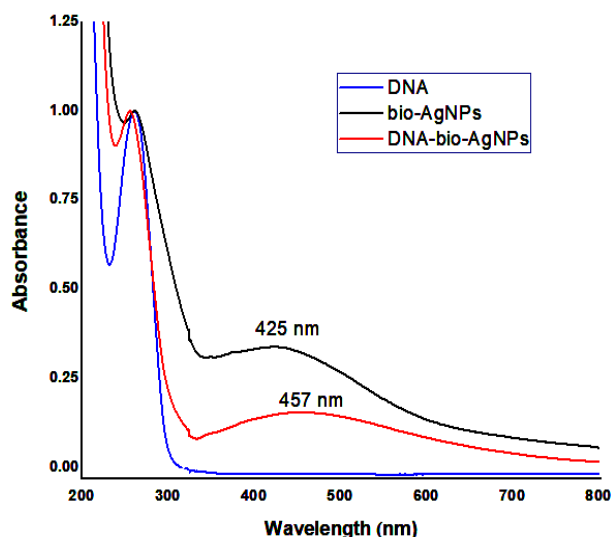


Fig. 5. Comparative presentation of UV-Vis absorption spectra (normalized at 260 nm) of herring DNA ( $7 \times 10^{-5}$  M), bio-AgNPs ( $5 \mu M$ ) and bio-complex DNA-bio-AgNPs (color online)

### 3.3. Estimation of bio-AgNPs effect on urease activity

Urease inhibitory effect of bio-AgNPs “green” synthesized in this study, was evaluated by electrical conductivity measurements, as described in the section 2.4. In the presence of AgNPs, a decrease of enzymatic reaction rate occurred. The percentage loss of ureolytic activity (%) (estimated as relative variation of hydrolysis rate, %) caused by bio-AgNPs, is depicted in Table 1. This urease inhibitory action could be due to the following reasons: (i) nanoparticle blocking the urease active site or (ii) urease conformational change [31].

These findings results are useful in the development of eco-friendly alternatives for conventional chemical methods, to design new materials based on “green” AgNPs for urease inhibitory action.

Table 1. The urease inhibitory action of bio-AgNPs

Sample set	C <sub>bio-AgNPs</sub> (mM)	Loss of ureolytic activity (%)
1	0	0
2	0.1	27
3	0.2	47

#### 4. Conclusions

In this paper, cornelian silver nanoparticles were phytosynthesized and assayed for new potential applications. The obtained AgNPs presented nanosize dimensions (with a mean diameter of 41.5 nm) estimated by DLS.

DNA binding studies were conducted in physiological conditions, by titrating increasing AgNPs amounts on DNA, and monitored by the UV-Vis absorption spectra. The results obtained from DNA binding assay could be exploited for DNA labelling to design novel drug delivery systems based on DNA or in biophotonic applications.

AgNPs “green” synthesized from *Cornus mas* fruits’ aqueous extract demonstrated urease inhibitory activity, so that these nanoparticles could be exploited as eco-friendly additives in urea-based fertilizers.

These results allow new potential applications of phytogenic silver nanoparticles in biophotonics and agriculture.

These findings are promising and stimulate further studies to develop novel complex eco-friendly formulations based on “green” AgNPs as platforms in biosensing and biophotonics, or in biomedical & agronomical fields.

#### Acknowledgements

The present study was supported by the Projects JINR – Romania: No. 48/2020 (Theme No.04-4-1121-2015/2020) and No. 75/2020 (Theme No. 04-4-1141-2020/2022) (IUCN ORDER no.269/20.05.2020) of JINR – Romania (University of Bucharest) collaboration.

#### References

- [1] A.-M. Manea-Saghin, C.-C. Pădurețu, F. Kajzar, *Opt. Mater.* **100**, 109669 (2020).
- [2] M. E. Barbinta-Patrascu, C. Ungureanu, N. Badea, M. Constantin, V. Purcar, A. Ispas, *J. Optoelectron. Adv. M.* **22**(5-6), 310 (2020).
- [3] M. E. Barbinta-Patrascu, N. Badea, C. Ungureanu, D. Besliu, S. Antohe, *Rom. Rep. Phys.* **72**(3), 606 (2020).
- [4] M. E. Barbinta-Patrascu, C. Ungureanu, N. Badea, M. Bacalum, A. Lazea-Stoyanova, I. Zgura, C. Negrila, M. Enculescu, C. Burnei, *Coatings* **10**, 659 (2020).
- [5] M. E. Barbinta-Patrascu, N. Badea, M. Bacalum, C. Ungureanu, I. R. Suica-Bunghez, S. M. Iordache, C. Pirvu, I. Zgura, V. A. Maraloiu, *Mater. Sci. Eng. C-Mater. Biol. Appl.* **101**, 120 (2019).
- [6] M. E. Barbinta-Patrascu, C. Ungureanu, I.-R. Suica-Bunghez, A.-M. Iordache, S. Milenković Petrović, A. Ispas, I. Zgura, *J. Optoelectron. Adv. M.* **20**(9-10), 551 (2018).
- [7] M. E. Barbinta-Patrascu, N. Badea, M. Constantin, C. Ungureanu, C. Nichita, S. M. Iordache, A. Vlad, S. Antohe, *Rom. J. Phys.* **63**(5-6), 702 (2018).
- [8] M. E. Barbinta-Patrascu, C. Ungureanu, S. M. Iordache, I. R. Bunghez, N. Badea, I. Rau, *J. Mater. Chem. B* **2**, 3221 (2014).
- [9] I. R. Bunghez, M. E. Barbinta-Patrascu, O. Dumitrescu, C. Ungureanu, I. Fierascu, S. M. Iordache, R. M. Ion, *Environ. Eng. Manag. J.* **15**(9), 2085 (2016).
- [10] M. E. Barbinta-Patrascu, *Optoelectron. Adv. Mat.* **13**(9-10), 546 (2019).
- [11] I. Rau, J. G. Grote, F. Kajzar, A. Pawlicka, *C. R. Physique* **13**, 853 (2012).
- [12] P. Gheorghe, A. Petris, V.I. Vlad, I. Rau, F. Kajzar, A. M. Manea, *Rom. Rep. Phys.* **67**(4), 1412 (2015).
- [13] A. Petris, P. Gheorghe, V. I. Vlad, I. Rau, F. Kajzar, *Rom. Rep. Phys.* **67**(4), 1373 (2015).
- [14] A. Petris, P. Gheorghe, I. Rau, A.-M. Manea-Saghin, F. Kajzar, *Eur. Polym. J.* **110**, 130 (2019).
- [15] M. E. Barbinta-Patrascu, N. Badea, C. Ungureanu, A. Ispas, *Optoelectron. Adv. M.* **13**(1-2), 131 (2019).
- [16] Z. Chen, C. Liu, F. Cao, J. Ren, X. Qu, *Chem. Soc. Rev.* **47**(11), 4017 (2018).
- [17] R. K. Thomas, S. Sukumaran, C. Sudarsanakumar, *J. Mol. Struct.* **1178**, 62 (2019).
- [18] R. K. Thomas, S. Sukumaran, C. Sudarsanakumar, *J. Mol. Liq.* **287**, 110911 (2019).
- [19] Y. Liu, C. Z. Huang, *Analyst* **137**, 3434 (2012).
- [20] K. Kappaun, A. R. Piovesan, C. R. Carlini, R. Ligabue-Braun, *J. Adv. Res.* **13**, 3 (2018).
- [21] H. Cantarella, R. Otto, J. R. Soares, A. G. de Brito Silva, *J. Adv. Res.* **13**, 19 (2018).
- [22] S. T. S. Hassan, E. Švajdlenka, *Molecules* **22**(10), 1696 (2017).
- [23] G. Mandalari, C. Bisignano, S. Cirmi, M. Navarra, *Evid.-based Complement Altern. Med.* **2017**, 8379262 (2017).
- [24] S. T. S. Hassan, E. Švajdlenka, K. R. R. Rengasamy, R. Melichárková, S. K. Pandian, *S. Afr. J. Bot.* **120**, 175 (2019).
- [25] L. V. Modolo, C. J. da-Silva, D. S. Brandão, I. S. Chaves, *J. Adv. Res.* **13**, 29 (2018).
- [26] V. Purcar, R. Somoghi, S. G. Nițu, C.-A. Nicolae, E. Alexandrescu, I. C. Gîfu, A. R. Gabor, H. Stroescu, R. Ianchiș, S. Căprărescu, L. O. Cinteza, *Nanomaterials* **7**, 439 (2017).

- [27] S. Roy, T. K. Das, *J. Nanosci. Nanotechnol.* **14**, 4899 (2014).
- [28] S. Pramanik, S. Chatterjee, A. Saha, P. S. Devi, G. Suresh Kumar, *J. Phys. Chem. B* **120**(24), 5313 (2016).
- [29] P. V. Subramanian, M. S. AlSalhi, S. Devanesan, P. A. Thomas, *J. Clust. Sci.* (2020).
- [30] M. E. Barbinta-Patrascu, A. M. Iordache, *Optoelectron. Adv. Mat.* **13**(11-12), 624 (2019).
- [31] S. Ponnuel, B. Subramanian, K. Ponnuraj, *The Protein Journal* **34**(5), 329 (2015).

---

\*Corresponding author: elipatras@gmail.com